Advanced Composite Materials
Publication details, including instructions for authors and subscription information:
http://www.tandfonline.com/loi/tacm20

Correlation of damage resistance under low velocity impact and Mode II delamination resistance in CFRP laminates

Iton Chou [a] , Toshihiro Inutake [b] & Kazuro Namba [c]
[a] Structure and Strength Department, Research Institute, Ishikawajima-Harima Heavy Industries Co., Ltd., 3-1-15, Toyosu, Koto-ku, Tokyo 135-8732, Japan
[b] Ishikawajima Inspection and Instrumentation Co., Ltd., 9-4, Fukuura, 1-chome, Kanazawa-ku, Yokohama 236-0004, Japan
[c] Composites Laboratory, Research Institute, Ishikawajima-Harima Heavy Industries Co., Ltd., 1, Shin-nakahara-cho, Isogo-ku, Yokohama 235-8501, Japan
Version of record first published: 02 Apr 2012.

To cite this article: Iton Chou , Toshihiro Inutake & Kazuro Namba (1999): Correlation of damage resistance under low velocity impact and Mode II delamination resistance in CFRP laminates, Advanced Composite Materials, 8:2, 167-176

To link to this article: http://dx.doi.org/10.1163/156855199X00173

Adv. Composite Mater., Vol. 8, No. 2, pp. 167–176 (1999)

Correlation of damage resistance under low velocity impact and Mode II delamination resistance in CFRP laminates

ITON CHOU [1,*], TOSHIHIRO INUTAKE [2] and KAZURO NAMBA [3]

[1] *Structure and Strength Department, Research Institute, Ishikawajima-Harima Heavy Industries Co., Ltd., 3-1-15, Toyosu, Koto-ku, Tokyo 135-8732, Japan*
[2] *Ishikawajima Inspection and Instrumentation Co., Ltd., 9-4, Fukuura, 1-chome, Kanazawa-ku, Yokohama 236-0004, Japan*
[3] *Composites Laboratory, Research Institute, Ishikawajima-Harima Heavy Industries Co., Ltd., 1, Shin-nakahara-cho, Isogo-ku, Yokohama 235-8501, Japan*

Received 6 July 1998; accepted 18 August 1998

Abstract—Investigated in this study was the correlation of the damage resistance under low velocity impact and Mode II interlaminar fracture toughness in five material systems, namely, T800/3631 (CF/Epoxy), UT500/PEEK (CF/PEEK), AS4/PEEK (CF/PEEK), IM7/PIX-A (CF/Polyimide) and T800/3900-2 (CF/Toughened Epoxy). These materials can be roughly divided into two types. One is a compatible type, which shows high impact resistance under low velocities with high Mode II delamination resistance. The other type is a non-compatible type, which has poor impact resistance at low velocities, even though it has superior Mode II delamination resistance. As for the system of T800/3631, T800/3900-2 and IM7/PIX-A composites, the Impact Energy (IE)/Damage Area (DA) ratio correlates well with $G_{\mathrm{IIC}}(0:P_{\mathrm{MAX}})$, Mode II energy release rate characterized at P_{MAX}, and $G_{\mathrm{IIR}}(0)$, Mode II energy release rate in propagation, for the 0/0 interface. The system of these materials is the compatible type. On the other hand, as for the system of T800/3631, UT500/PEEK and AS4/PEEK composites, the IE/DA ratio correlates well with $G_{\mathrm{IIC}}(P_{\mathrm{NL}})$, Mode II energy release rate characterized at P_{NL}, for 0/0 and 22.5/−22.5 interfaces. The system of these materials is the non-compatible type. It is suggested that the main reason for the difference in behavior of these two types is that the compatible type has the superior Mode II delamination resistance in the sub-critical crack growth region and propagation. It correlates with the superior impact resistance under low velocities.

Keywords: Impact; delamination; damage resistance; Mode II; toughness; low velocity; correlation.

*To whom correspondence should be addressed. E-mail: iton_chou@ihi.co.jp

1. INTRODUCTION

In laminated composites used for aerospace structures, delaminations often occur as a result of impact at low and high velocities. Especially for the application of laminated composites to components of aeronautical turbo engines, impact damage resistance is therefore a primary design issue.

Morita *et al.* [1, 2] reported the damage resistance of CF/PEEK and CF/Toughened Epoxy laminates under low and high velocity impact tests. The report clarified that the relation between damage area (DA) and impact energy (IE) was linear, and the ratio DA/IE indicated the impact resistance for each specimen. Moreover, they reported that a ranking of impact resistance could be obtained both relatively and quantitatively among material systems tested in the work, and the ranking was dependent on impact velocity level.

Masters [3] and Odagiri *et al.* [4] investigated the correlation of Compression After Impact (CAI) strength and Mode II interlaminar fracture toughness in CFRP laminates. The work indicated that CAI strength could be estimated from Mode II interlaminar fracture toughness. The concept of CAI strength is introduced in the design of airplane frames. However, the CAI strength is not usually used in designing of aeronautical turbo engines. It is desirable for the screening and selection of laminated composites in the designing to use a simple material property.

For this reason, investigated in this study was the correlation of the damage resistance under low velocity impact and Mode II interlaminar fracture toughness in five material systems, namely, T800/3631 (CF/Epoxy), UT500/PEEK (CF/PEEK), AS4/PEEK (CF/PEEK), IM7/PIX-A (CF/Polyimide), and T800/3900-2 (CF/Toughened Epoxy). This work consisted of three steps. The first step was to measure the damage resistance under low velocity impact of these material systems. The second step was to measure Mode II interlaminar fracture toughness of the laminates by conducting the End Notched Flexure (ENF) test. The final step was to correlate the results obtained from low velocity impact tests and ENF tests.

2. EXPERIMENTAL DETAILS

2.1. Materials and specimen geometry

Five material systems, T800/3631 (CF/Epoxy, TORAY), UT500/PEEK (CF/Poly-Ether-Ether-Ketone, TOHO RAYON), AS4/PEEK (CF/Poly-Ether-Ether-Ketone, FIBERITE), IM7/PIX-A (CF/Polyimide, MITSUI CHEMICAL), and T800/3900-2 (CF/Toughened Epoxy, TORAY) were employed to measure the low impact resistance and Mode II interlaminar fracture toughness in this study. Unidirectional prepregs were used to fabricate flat panels for test specimens. These panels were fabricated in an autoclave, and test specimens were cut out from each panel. Impact test specimens were basically quasi-isotropic laminates. The stacking sequence of test specimens is shown in Table 1. In this study, the number

Table 1.
Stacking sequences of test specimens

Materials	ENF test specimens		Impact test specimens
	0/0	22.5/−22.5	
T800/3631	$[0_{12}/\mathrm{IF}/0_{12}]^b$	*a*	$[0_3/45_3/90_3/-45_3]\mathrm{s}$
UT500/PEEK	$[0_{12}/\mathrm{IF}/0_{12}]$	*a*	$[0_3/45_3/90_3/-45_3]\mathrm{s}$
AS4/PEEK	$[0_{12}/\mathrm{IF}/0_{12}]$	*a*	$[0_3/45_3/90_3/-45_3]\mathrm{s}^c$
IM7/PIX-A	$[0_{12}/\mathrm{IF}/0_{12}]$	*a*	$[0_3/45_3/90_3/-45_3]\mathrm{s}$
T800/3900-2	$[0_8/\mathrm{IF}/0_8]^b$	Not fabricated	$[0_2/45_2/90_2/-45_2]\mathrm{s}^c$

[a] $[22.5/-22.5/0_8/-22.5/22.5/\mathrm{IF}/-22.5/22.5/0_8/22.5/-22.5]$, IF: Inserted Film.
[b] Referred to [5, 6].
[c] Referred to [1, 2].

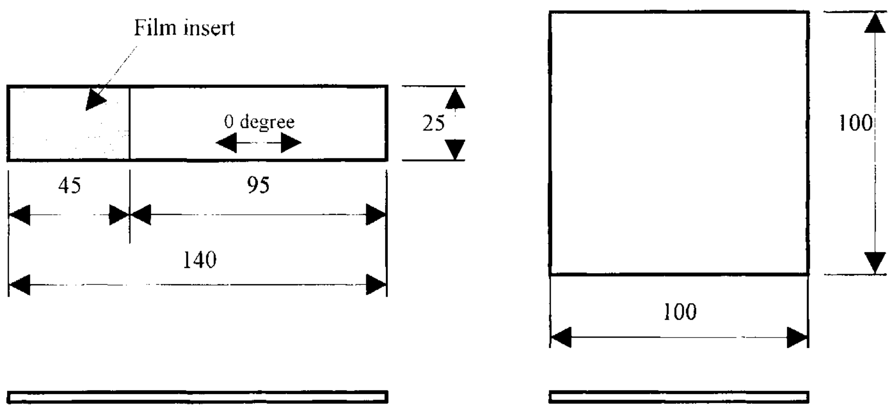

(a) ENF Test Specimen (b) Impact Test Specimen

Figure 1. Specimen geometry (unit in mm).

of 0, 45, −45, and 90 degree plies was selected to be 2 or 3 in order to simplify the delamination problem, since the fracture of test specimens was complicated when only one ply number was selected. ENF test specimens were stacked in two ways. One was the unidirectional stacking to measure Mode II interlaminar fracture toughness at the 0/0 interface. The other was a special stacking, such as $[22.5/-22.5/0_8/-22.5/22.5/\mathrm{IF}/-22.5/22.5/0_8/22.5/-22.5]$ according to the author's report [5, 6], in order to measure Mode II energy release rate at the 22.5/−22.5 interface. Here, IF in the stacking sequence represents the inserting film (a 7.5 μm thick Kapton film) as a pre-crack. Specimen geometry is shown in Fig. 1.

2.2. Impact test procedure

An instrumented drop weight impactor (Dynatup GRC-8250 system) consisting of a 2.53 kg striker with 12.7 mm diameter mild steel hemispherical tip was used for the low velocity impact test. The test specimen was clamped between the two square frame plates that have a central circular cutout with a diameter of 76.2 mm, and set between the plates so as to be impacted at the center of the plate. In addition, the test specimen was clamped at the four corners of the square frame plates under the condition of constant clamping force for each corner. The boundary condition of clamping for the specimen can be considered the condition between a rigid support and a simple support. Impact velocities were measured with a photoelectric detector. The incident impact energy on specimens was changed by varying the drop height. Impact velocity ranged from 1.3 to 3.6 m/s and incident energy ranged from 2 to 16 J. After impact testing, the specimens were evaluated for the damage profile and projected area using an ultrasonic C-Scan system (HITACHI AT-3000) with a 10 MHz transducer.

2.3. ENF test procedure

The ENF test was used to measure Mode II energy release rate at 0/0 and 22.5/−22.5 interfaces. The test was conducted according to Japanese Industrial Standard, 'Testing Methods for Interlaminar Fracture Toughness of Carbon Fiber Reinforced Plastics' (JIS K-7086 in the English version). Tests were performed with a constant crosshead rate of 2 mm/min. The span length was 100 mm. During testing, an approximately 360-μm thick film with a width of 10 mm was inserted between the upper and lower beams of the ENF specimen at the supporting nose of the delaminated end to decrease the friction between the fracture surfaces. The initial crack length was directly measured from the fracture surface of each specimen broken in two pieces in Mode I propagation after testing.

Before performing the ENF test, each specimen was wedged open to ensure the debonding between the fracture surfaces and the inserted film. Precracks were not introduced and the precrack length was 25 mm.

3. RESULTS AND DISCUSSION

3.1. Impact test results

Figure 2 shows the relation between Impact Energy (IE) and Damage Area (DA) in T800/3631, UT500/PEEK, AS4/PEEK, IM7/PIX-A, and T800/3900-2 composites. Here, the absorbed energy is selected for the Impact Energy (IE). In addition, the Damage Area (DA) is the projected damage area. The best fit lines calculated by the least squares method are also shown in Fig. 2. It is clear from the result that the relation is linear and the ratio of IE/DA can be obtained from every material system by the least square linear fit. IE/DA ratios for the material systems are summarized in Table 2.

Table 2.
Summary of Mode II interlaminar fracture toughness and IE/DA ratios

Material systems	Items	Mode II interlaminar fracture toughness								Impact property
		0/0				22.5/−22.5				
		G_{IIC}			G_{IIR}	G_{IIC}			G_{IIR}	IE/DA
		P_{NL}	$P5$	P_{MAX}		P_{NL}	$P5$	P_{MAX}		
T800/3631	Mean (kJ/m^2)	0.242	0.507	0.514	0.645	0.297	0.558	0.558	0.689	1.758
	C.O.V.[a]	0.059	0.012	0.011	0.037	0.091	0.069	0.069	0.040	—
	n[b]	5	5	5	10	6	6	6	12	9
UT500/PEEK	Mean (kJ/m^2)	0.403	1.500	1.602	2.041	0.359	1.355	1.435	1.696	1.966
	C.O.V.	0.108	0.105	0.065	0.077	0.102	0.141	0.186	0.125	—
	n	4	4	4	7	6	6	6	12	15
AS4/PEEK	Mean (kJ/m^2)	0.952	1.880	1.949	2.276	0.729	2.621	2.998	3.492	3.734
	C.O.V.	0.082	0.062	0.067	0.080	0.097	0.047	0.032	0.054	—
	n	5	5	5	10	6	6	6	12	12
IM7/PIX-A	Mean (kJ/m^2)	0.659	2.194	2.369	2.688	0.502	2.221	2.940	3.216	16.973
	C.O.V.	0.119	0.037	0.047	0.038	0.204	0.092	0.082	0.085	—
	n	5	5	5	10	6	6	6	12	12
T800/3900-2	Mean (kJ/m^2)	0.280	1.123	1.625	1.972	—	—	—	—	10.013
	C.O.V.	0.093	0.203	0.104	0.113	—	—	—	—	—
	n	5	5	5	10	—	—	—	—	12

[a] Coefficients of variation.
[b] Number of specimens for G_{IIC} and the impact property; number of data for G_{IIR}.

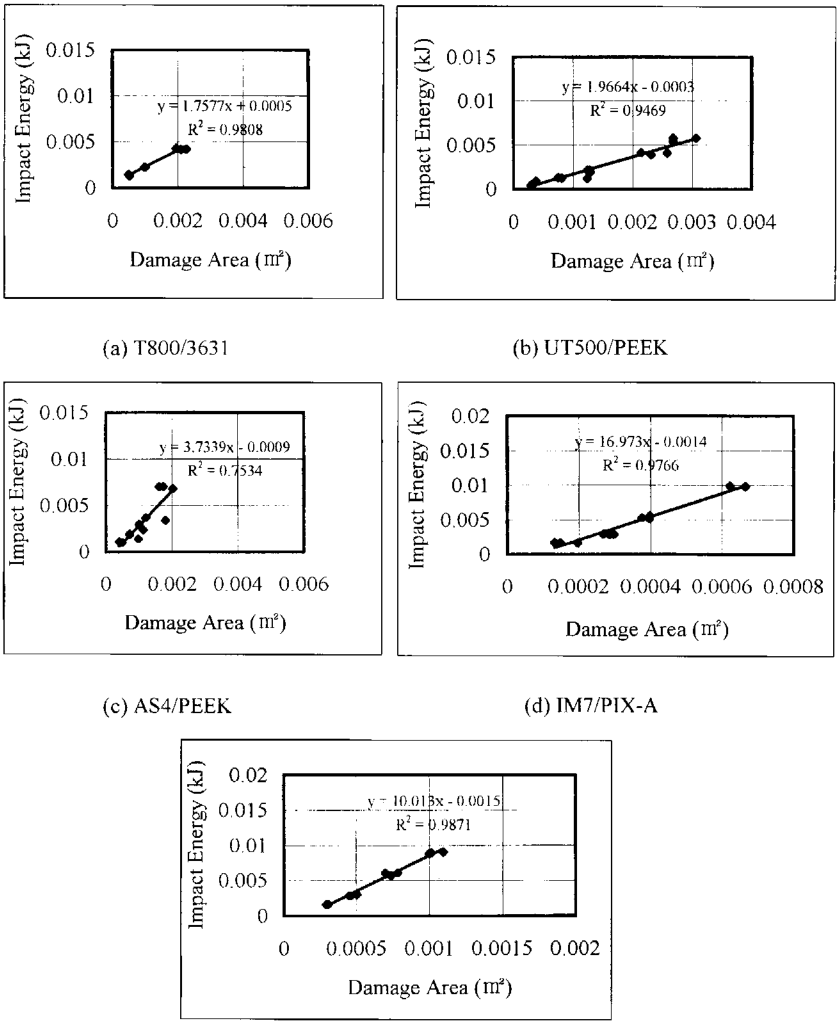

(a) T800/3631 (b) UT500/PEEK (c) AS4/PEEK (d) IM7/PIX-A (e) T800/3900-2

Figure 2. Relation between Impact Energy (IE) and Damage Area (DA) for each material system.

3.2. ENF test results

In this study, Mode II energy release rate at crack initiation, G_{IIC}, was characterized using three load values. One was P_{NL}, the loading point which corresponded to the onset of nonlinear response in the load versus load line displacement curve. Another one was $P5$, the loading point which corresponded to the intersection of the 5% secant line (5% offset line) and the load versus load line displacement curve. The remaining one was P_{MAX}, the maximum loading point. For the small non-linearity, $P5$ was considered equal to P_{MAX}. G_{IIC} characterized at $P5$ and P_{MAX} were calculated using the corrected crack length which can be determined by the initial crack length according to the equation for correction described in JIS K-7086. Mode II energy release rate in propagation, G_{IIR}, was also calculated.

Table 2 summarizes G_{IIC} and G_{IIR} at 0/0 and 22.5/−22.5 interfaces obtained from ENF tests and the ratios of IE/DA obtained from low velocity impact tests. G_{IIR} shown in Table 2 represents the mean value of G_{IIR} in the range of 10 to 20 mm crack extension. G_{IIC} and G_{IIR} at 0/0 and 22.5/−22.5 interfaces were compared with the ratio IE/DA for each material system using the data shown in Table 2.

3.3. Correlation of IE/DA ratios and G_{IIC}/G_{IIR}

Figure 3 shows the relation between IE/DA ratios and $G_{IIC}(22.5 : P_{NL})$, G_{IIC} at the 22.5/−22.5 interface characterized at P_{NL} for three material systems of T800/3631, UT500/PEEK and AS4/PEEK. Figure 3 also shows the relation between IE/DA ratios and $G_{IIC}(0 : P_{NL})$, G_{IIC} at the 0/0 interface characterized at P_{NL}. In the figure, best fit lines calculated by the least squares method are also plotted. The correlation coefficient of the fitted line for the 0/0 interface is about 0.98 and that for the 22.5/−22.5 interface is about 0.99. It is obvious that the relation between the ratio IE/DA and $G_{IIC}(22.5 : P_{NL})$ or $G_{IIC}(0 : P_{NL})$ is linear for these material systems. It means that the ratio IE/DA can be estimated by $G_{IIC}(0 : P_{NL})$ data. In other words, the damage resistance under low velocity impact can be estimated by conducting the conventional ENF test [7].

Figure 4 shows the relation between IE/DA ratios and $G_{IIC}(0 : P_{MAX})$, G_{IIC} at the 0/0 interface characterized at P_{MAX}, for five material systems tested in this study. In addition to these, the relation between IE/DA ratios and $G_{IIR}(0)$, G_{IIR} at the 0/0 interface, for the five material systems are shown in Fig. 5. It is clear from Figs 4 and 5 that the ratio IE/DA does not correlate with $G_{IIC}(0 : P_{MAX})$ and

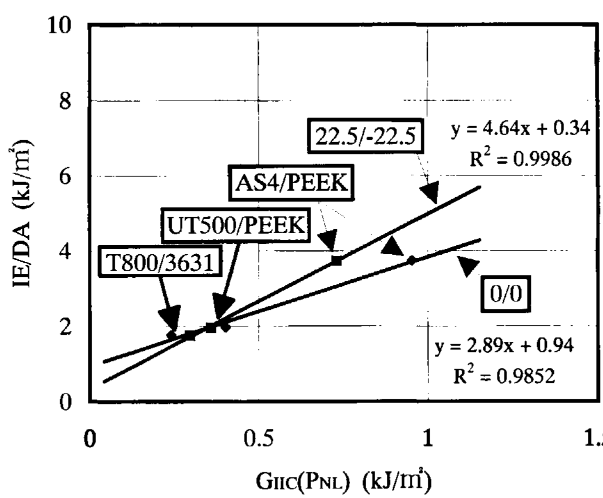

Figure 3. Relation between IE/DA ratios and $G_{IIC}(P_{NL})$, Mode II energy release rate characterized at P_{NL}.

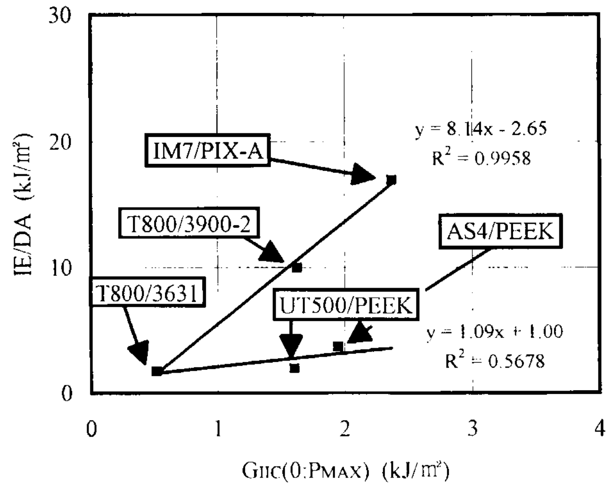

Figure 4. Relation between IE/DA ratios and $G_{IIC}(0 : P_{MAX})$, Mode II energy release rate at the 0/0 interface when they are characterized at P_{MAX}.

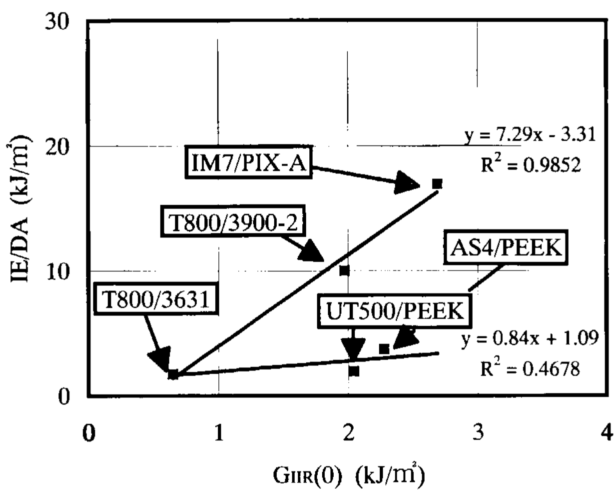

Figure 5. Relation between IE/DA ratios and $G_{IIR}(0)$, mean value of Mode II energy release rate at the 0/0 interface in propagation.

$G_{IIR}(0)$ for the system of T800/3631, UT500/PEEK and AS4/PEEK composites. Moreover, the slope of the fitted line for these materials is small. In contrast, the ratio IE/DA correlates with $G_{IIC}(0 : P_{MAX})$ and $G_{IIR}(0)$ for the system of T800/3631, T800/3900-2, and IM7/PIX-A composites. The slope of the fitted line for this system is larger than that for the former system, that is the system of T800/3631, UT500/PEEK, and AS4/PEEK composites. These facts indicate that material systems tested in this study can be roughly divided into two types. One is a compatible type, that is T800/3900-2 and IM7/PIX-A systems. This type shows high impact resistance under low velocities and high Mode II delamination resistance. The other type is a non-compatible type, that is UT500/PEEK and AS4/PEEK systems. This type has poor impact resistance under low velocities, even though it has superior Mode II delamination resistance.

The reasons why the materials evaluated in this study may be divided into two types, that is the compatible type and the non-compatible one, can be explained by the following. In Figs 4 and 5, it can be recognized that the ratio IE/DA correlates well with $G_{IIC}(0 : P_{MAX})$ and $G_{IIR}(0)$ for the system of T800/3631, T800/3900-2 and IM7/PIX-A composites. Also, the slope of fitted lines for this system in Figs 4 and 5 is large. These facts mean that the impact resistance under low velocities correlates well with the Mode II delamination resistance in the sub-critical crack growth and propagation stage for the system of T800/3631, T800/3900-2 and IM7/PIX-A composites. The compatible type, such as T800/3900-2 and IM7/PIX-A composites, has the superior Mode II delamination resistance in the sub-critical crack growth and propagation stage. In addition, the superior Mode II delamination resistance in the sub-critical crack growth and propagation stage correlates well with the superior impact resistance under low velocities. The superior delamination resistance under the static Mode II is compatible with that under the low velocity impact for this material type. This is called the compatible type in this study. On the other hand, it can be recognized in Figs 4 and 5 that the ratio IE/DA does not correlate with $G_{IIC}(0 : P_{MAX})$ and $G_{IIR}(0)$ for the system of T800/3631, UT500/PEEK and AS4/PEEK composites, although the ratio IE/DA correlates well with G_{IIC} characterized at P_{NL} as shown in Fig. 3. Also, the slope of fitted lines for this system shown in Figs 4 and 5 is small. These experimental facts indicate that the superior Mode II delamination resistance does not lead to superior impact resistance under low velocities. In other words, the superior delamination resistance under the static Mode II is not compatible with that under the low velocity impact for this material type. This is called the non-compatible type in this study.

In addition to the experimental results described above, further study regarding the micro-mechanism of the delaminations under the static Mode II and the low velocity impact for these materials is required in order to examine the difference between these two material types. Also, further study on other material systems, especially on an interleaved system and a toughened system, is required.

4. CONCLUSIONS

Results obtained in this study can be summarized in the following.

(1) Material systems investigated in this study can be roughly divided into two types. One is a compatible type, which combines high impact resistance under low velocities and high Mode II delamination resistance. The other type is a non-compatible type, which has poor impact resistance under low velocities, even though it has superior Mode II delamination resistance.

(2) As for the system of T800/3631, T800/3900-2 and IM7/PIX-A composites, the IE/DA ratio correlates well with $G_{IIC}(0 : P_{MAX})$ and $G_{IIR}(0)$ for the 0/0 interface. The slope of the fitted line in the relation between the IE/DA ratio and G_{II} is large. The material system like T800/3900-2 and IM7/PIX-A composites is the compatible type.

(3) As for the system of T800/3631, UT500/PEEK and AS4/PEEK composites, the IE/DA ratio correlates well with $G_{IIC}(P_{NL})$ for 0/0 and 22.5/−22.5 interfaces. However, the IE/DA ratio does not correlate with $G_{IIC}(0 : P_{MAX})$ and $G_{IIR}(0)$. The slope of the fitted line in the relation between the IE/DA ratio and G_{II} is small. The material system like UT500/PEEK and AS4/PEEK composites is the non-compatible type.

Further study regarding the micro-mechanism of the delaminations under the static Mode II and the low velocity impact for these materials is required in order to examine the difference between the compatible type and the non-compatible one. Also, further study on other material systems, especially on an interleaved system and a toughened system, is required in addition to the result described in this paper.

Acknowledgements

The authors would like to thank Dr. Morita, in the Composites Laboratory of IHI, for the technical assistance of an ultrasonic C-Scan and useful discussion. Mr. Hirose, in the Composites Laboratory of IHI, is also gratefully acknowledged for his assistance in specimen fabrication.

REFERENCES

1. H. Morita, T. Adachi, Y. Tateishi and H. Matsumoto, Characterization of impact damage resistance of CF/PEEK and CF/toughened epoxy laminates under low and high velocity impact tests, *J. Reinf. Plast. Compos.* **2**, 131–143 (1997).
2. H. Morita, T. Adachi, H. Matsumoto and P. H. W. Tsang, Effects of impact conditions and stacking sequence on impact damage in CF/PEEK laminates, *Trans. Jpn Soc. Mech. Eng.* **613A**, 203–209 (1997) (in Japanese).
3. J. E. Masters, Correlation of impact and delamination resistance in interleafed laminates, in: *Proc. ICCM-VI & ECCM-2*, Vol. 3, pp. 96–107 (1987).
4. N. Odagiri, T. Muraki and K. Tobukuro, Toughness improved high performance TORAYCA prepreg T800H/3900 series, in: *Proc. Intern. SAMPE Symp. and Exhibition*, G. Carrillo, E. D. Newell, W. D. Brown and P. Phelan (Eds), pp. 272–283 (1988).
5. I. Chou, I. Kimpara, K. Kageyama and I. Ohsawa, Mode I and Mode II fracture toughness measured between differently oriented plies in graphite/epoxy composites, in: *ASTM STP 1230*, R. H. Martin (Ed.), pp. 132–151. American Society for Testing and Materials, Philadelphia (1995).
6. I. Chou, Research on factors affecting on the interlaminar fracture toughness in carbon fiber reinforced plastics, Doctoral dissertation, University of Tokyo (1996) (in Japanese).
7. I. Chou and K. Namba, Correlation of damage resistance under low velocity impact and Mode II interlaminar fracture toughness in CFRP laminates, in: *Proc. 8th Japan–US Conf. Compos. Mater.*, G. M. Newaz and R. F. Gibson (Eds), pp. 459–466 (1998).